Advances in Materials Research, *Vol.3, No.2 (2014) 105-116*
DOI: http://dx.doi.org/10.12989/amr.2014.3.2.105

Cryogenic microwave dielectric properties of Mg_2TiO_4ceramics added with CeO_2nanoparticles

Ranjan K. Bhuyan[1], Santhosh K. Thatikonda[1], Pamu Dobbidi[1], J.M. Renehan[2] and Mohan V. Jacob[*2]

[1]*Department of physics, Indian Institute of Technology Guwahati, Guwahati -39, India*
[2]*Electronics Materials Lab., School of Engineering and Physical Sciences, James Cook University, Townsville, QLD 4811 Australia*

(Received February 10, 2014, Revised July 9, Accepted July 10, 2014)

Abstract. The microwave dielectric properties of CeO_2 nanoparticles (0.5, 1.0 & 1.5wt%) doped Mg_2TiO_4 (MTO) ceramics have been investigated at cryogenic temperatures. The XRD patterns of the samples were refined using the full proof program reveal the inverse spinel structure without any secondary phases. The addition of CeO_2 nanoparticles lowered the sintering temperature with enhancement in density and grain size as compared to pure MTO ceramics. This is attributed to the higher sintering velocity of the fine particles. Further, the microwave dielectric properties of the MTO ceramics were measured at cryogenic temperatures in the temperature range of 6.5-295 K. It is observed that the loss tangent (tanδ) of all the samples increased with temperature. However, the CeO_2 nanoparticles doped MTO ceramics manifested lower loss tangents as compared to the pure MTO ceramics. The loss tangents of the pure and MTO ceramics doped with 1.5 wt% of CeO_2 nanoparticles measured at 6.5K are found to be 6.6×10-5 and 5.4×10-5, respectively. The addition of CeO_2 nanoparticles did not cause any changes on the temperature stability of the MTO ceramics at cryogenic temperatures. On the other hand, the temperature coefficient of the permittivity increased with rise in temperature and with the wt% of CeO_2 nanoparticles. The obtained lower loss tangent values at cryogenic temperatures can be attributed to the decrease in both intrinsic and extrinsic losses in the MTO ceramics.

Keywords: cyogenic temperatures; microwave dielectric properties; CeO_2 nanoparticles; densification, microstructure

1. Introduction

The tremendous growth in telecommunication and satellite broadcasting has resulted in a need for low loss and low cost high frequency devices, such as, dielectric resonator and dielectric filters. The dielectric resonator provides the compactness, light weight, temperature stability (due to the lower temperature coefficient of resonant frequency), miniaturization (due to a high dielectric constant), and high-frequency selectivity. The dielectric resonators with a high dielectric constant (ε_r), a low loss (large $Q\times f_o$) and a temperature coefficient of resonant frequency (τ_f) are used in filters, oscillators, amplifiers and tuners in communication circuits, which results in the high

∗Corresponding Author, Professor, E-mail: - mohan.Jacob@jcu.edu.au

http://www.techno-press.org/?journal=amr&subpage=7 ISSN: 2234-0912 (Print), 2234-179X (Online)

demand for dielectric resonators with superior dielectric materials (Freer and Azough 2008, Chen 2012, Reaney and Iddles 2006).

Magnesium Titanate (Mg_2TiO_4) has the potential to be one of the best and promising microwave resonator materials for microwave applications, due to its excellent dielectric properties ($\varepsilon_r \approx 14$, τ_f −50 ppm/◦C and $Q \times f_0 = 150{,}000$ at 10 GHz) (Belous *et al*. 2007, Huang *et al*. 2009). However, due to the relatively high sintering temperature (1450^{o}C) of MTO ceramics it is difficult to densify the material at lower sintering temperatures without a sintering aid. To reduce the processing temperature, whilst improving the density and microstructure of MTO ceramics, this study chose cerium (IV) oxide (CeO_2) nanoparticles as the sintering aid. CeO_2 nanoparticles have tremendous surface to volume ratios, which modifies the microstructure and enhances the diffusion during the sintering process. Higher densities can be achieved by the addition of nanoparticles at lower temperatures over shorter time scales.

The dielectric loss is the factor that primarily limits the use of dielectric resonator materials in microwave devices (Kuang *et al*. 2006, Jacob *et al*. 2006). An efficient use of material in these devices necessitates the understanding nature of dielectric loss. Minimization of the dielectric loss is one of the important tasks for improving the material performance. Thus, it is important to comprehend the fundamental mechanism of the dielectric loss at microwave frequencies. In general, the microwave dielectric loss originates from intrinsic and extrinsic loss mechanisms (Ferreira *et al*. 1993). The intrinsic loss occurs primarily due to the anharmonicities of the lattice vibration, and the extrinsic loss is associated to factors such as impurities, secondary phases, non-uniform grain growth and porosity. However, there is no clear understanding of the mechanisms themselves as well as the relationships between these mechanisms. Dielectric measurements at cryogenic temperatures can provide important insights about the dynamics of molecular and ionic matter, which allows advancement in the understanding the intrinsic loss mechanisms (Pamu *et al*. 2007, Subodh *et al*. 2008).

Cryogenic electronics is a rapid development branch of emerging electronics, remarkably to understand the low temperature and fundamental properties. Furthermore, most of the conventional mobile communication equipment operates between -25^{o}C and 50^{o}C. Hence, it is important to characterize the dielectric properties of materials and their variation with temperature before using them. Successful design and manufacture of low-loss devices require the use of components with a high Q factor and the lowest loss at cryogenic temperatures. To achieve this, the meticulous choice of dielectric materials is needed for their fabrication. In order to find suitablematerials for cryogenic electronic devices, the microwave dielectric property at cryogenic temperatures is necessary. Currently, there is very minimal data available concerning the dielectric properties of microwave materials at cryogenic temperatures. Hence it has motivated us to study and understand the microwave dielectric properties of the MTO ceramics at cryogenic temperatures.

In this paper, the microwave dielectric properties of pure MTO ceramics and doped MTO ceramics with different concentrations of CeO_2 nanoparticles at cryogenic temperatures is measured and reported.

2. Experimental procedure

MTOceramics were synthesized by conventional solid-state reaction method from individual high-purity oxide powders (99.99%, Sigma Aldrich) Magnesium Oxide (MgO) and Titanium Dioxide (TiO_2). The starting materials were mixed in accordance with the desired stoichiometry of the MTO ceramics. The powders were ground in distilled water for 1 hour by using a planetary

ball mill (Fritsch, GmBH, Germany). The milled powders were calcined at 900^{o}C for 3 hours, and the calcinated powders were re-milled for 10 hours. Subsequently, a different weight percent of CeO_2 nanoparticles (0, 0.5, 1.0 and 1.5) was added to the milled powders and further milled for 1 hour. Finally, the as-milled powders were uniaxially pressed into pellets with dimensions of 10 mm in diameter and 4 - 5mm in thickness under a pressure of 200 MPa. The samples were sintered at 1250 - 1400^{o}C for 3 hours. The heating and cooling rates were set as 10^{o}C/min and 2^{o}C/min, respectively.

The crystalline phases of the MTO ceramics were identified from the X-Ray diffraction pattern (Rigaku TTRAX 18 KW, Cu-$K_\alpha$radiation) and the densities of the sintered MTO ceramics were measured by Archimedes's method. The surface morphology was analyzed by scanning electron microscopy (SEM, LEO 1430-VP). The experimental technique used for the microwave characterization is thoroughly discussed elsewhere (Jacob *et al*. 2008, Jacob 2005). The experimental system consists of Vector Network Analyzer (E8356B, Agilent Technology, Palo Alto, CA), a closed-cycle refrigerator (ARS Cryo), a temperature controller (LTC 340, Lakeshore, CA), Custom made vacuum dewar, PC, and a TE_{011} mode dielectric resonator. The resonator containing the dielectric material was cooled from room temperature to approximately 6.5 K. The TE_{011} mode resonance is identified around 10 GHz. The S_{21}, S_{11}, and S_{22} parameter data around the resonance were measured at the lowest temperature. The Transmission Mode Q-Factor (TMQF) technique (Ginzton 1995) has been used to eliminate all kinds of parasitic losses and to precisely compute coupling coefficients k_1 and k_2 (Jacob *et al*. 2001). The S_{21} parameter is measured as a function of temperature from 6.5 to 295 K. The coupling coefficient for each measurement temperature is calculated using a simplified TMQF and hence the unloaded Q factor. The perpendicular component of the real part of the relative permittivity and loss tangent (tanδ) of MTO was computed from the measured resonant frequency and calculated unloaded Q factor, respectively.

3. Results and discussions:

3.1 X-ray diffraction and Rietveld refinement analysis

The effect of CeO_2 nanoparticles on the crystal structure of the MTO ceramics is studied by using the XRD patterns (Bhuyan *et al*. 2013). It was observed that both pure MTO and the MTO ceramics doped with CeO_2 nanoparticles revealed an inverse spinel structure and did not show any secondary phases up to 1.5 wt% CeO_2. Nevertheless, it is difficult to suppress the secondary phases such as $MgTiO_3$ and $MgTi_2O_5$ in the MTO ceramics prepared by solid-state reaction method. In contrast, in the present study, no appearance of such secondary phases is observed, and this may be due to the ball milling effect and smaller initial particle sizes.

Further, the XRD patterns of all samples could be refined by taking Fd-3m space group in cubic cell. The typical XRD Patterns along with the Rietveld refinement of pure MTO and MTO + 1.5 wt% CeO_2 nanoparticles sample sintered at 1400^{o}C and 1300^{o}C for 3 hours respectively, are shown in Fig. 1 (a & b). The refinement was carried out by varying cell parameters, position of the Mg, Ti, and O atoms, occupancy, and thermal parameters. The lattice constants of pure and MTO+ x wt % ceramics were calculated and are found to be approximately same for all samples. Hence, it indicates that CeO_2 nanoparticles are not forming a solid solution with MTO matrix but segregated

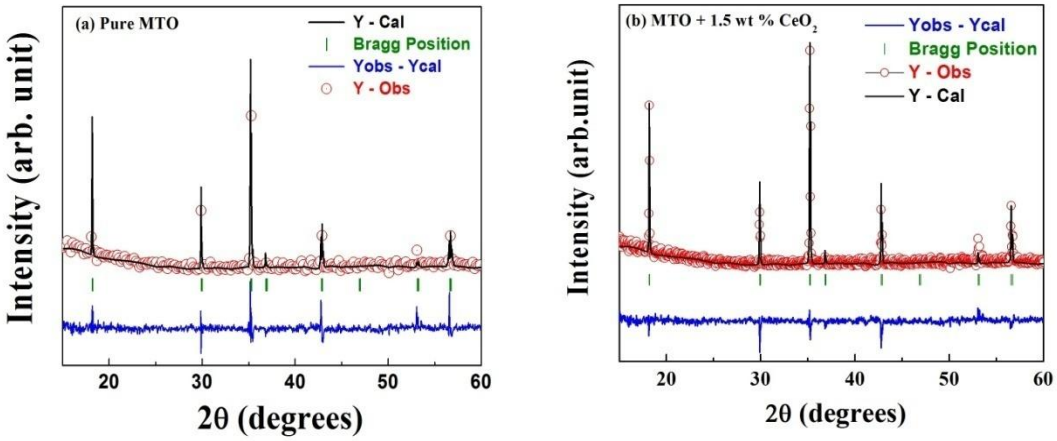

Fig. 1(a). XRD pattern along with Rietveld refinement of pure MTO ceramics sintered at 1400℃ and 1(b). MTO + 1.5 wt% CeO_2 nanoparticles sintered at 1300 ℃

Table 1 Parameters obtained from the Rietveld analysis of XRD patterns for MTO + 1.5 wt% CeO_2nanoparticles sample.χ^2 , R_{Brag} , R_f *are Reliability Factors*

Sample prameters	Pure MTO	MTO + 1.5 wt% CeO_2 nanoparticles
χ^2	1.00	0.666
R_{Brag}	14.57	12.46
R_f	12.07	11.84
a=b=c (Å)	8.4461 (12)	8.4462 (15)
Volume (Å ^{3})	602.51 (05)	602.53 24)

at the grain boundary. The refined parameters with lattice constants obtained from Rietveld analysis of the as prepared samples are given in Table 1. The derived lattice constant from Rietveld refinement was well set with the standard lattice constants of MTO ceramics prepared with solid-state reaction method. This is anticipated due to the differences in the ionic radii of Ce^{4+} ions (1.02 Å) as compared to Mg^{2+} (0.72 Å) and Ti $^{4+}$ (0.605 Å) ions. Therefore, the Ce^{4+} ion cannot be substituted in the Mg^{2+} and Ti $^{4+}$ sites.

3.2 Surface morphology

The influence of CeO_2 nanoparticles on the microstructure of the MTO ceramics is investigated using the SEM images shown in Fig. 2 (a-d), where (a) corresponds to pure MTO sintered at 1400^{o}C and (b-d) corresponds to 0.5-1.5 wt% CeO_2 nanoparticles, and sintered at 1300^{o}C, respectively. The SEM demonstrates the highly densified microstructures, and the samples crack free. Pure MTO ceramics displayed smaller grains compared with the samples with the added CeO_2 nanoparticles that may be attributed to the insufficient sintering temperature. CeO_2 doped MTO ceramics exhibited a homogeneous microstructure with large average grain sizes. The addition of CeO_2 nanoparticles not only improved the microstructure but also enhanced the relative

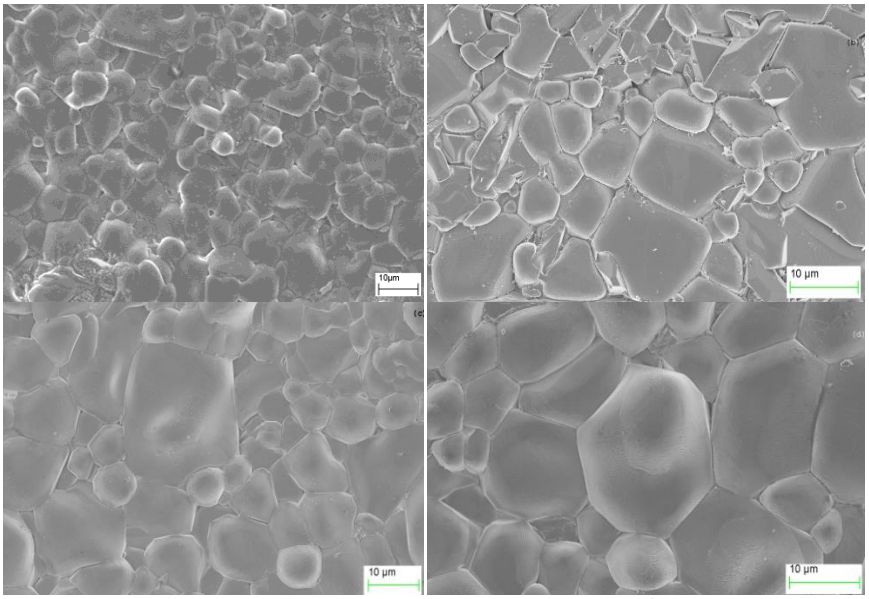

Fig 2 SEM images of the (a) Pure MTO ceramics sintered at 1400 ^{o}C and MTO+ *x* CeO_2 (*x* = *0.5-1.5* wt.%) ceramics with (b) 0.5 wt%, (c) 1.0 wt% and (d) 1.5 wt%, sintered at 1300^{o}C

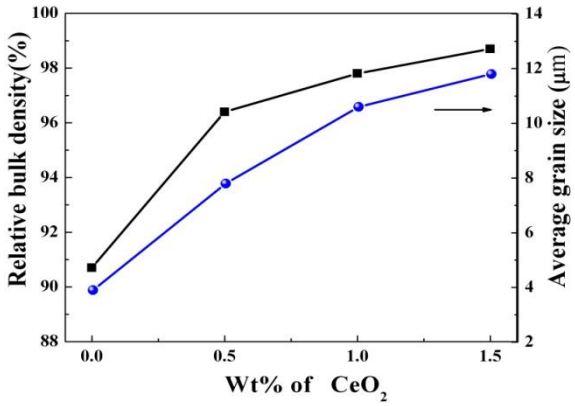

Fig. 3 Variation of relative density and average grain sizes as a function of wt% of CeO_2 sintered at 1300^{o}C

densities at lower sintering temperatures (at 1300^{o}C). The variation of density and average grain sizes as a function of wt% of CeO_2 nanoparticles, for the samples sintered at 1300°C for 3 h, is shown in Fig.3. It is observed that the relative density, and the average grain size of the samples enhanced with an increase in wt% of CeO_2 nanoparticles. The highest relative density of 98.7% is observed for the sample with 1.5 wt% of CeO_2, sintered at 1300℃ for 3 h. The improvement in the density associated with the addition of CeO_2 nanoparticles can be assigned to the smaller initial particle sizes, large surface area and the surface energy available for the nanoparticles. That means, smaller particles enhance the sintering velocity and the diffusion across the boundary increases. In addition, the surface-free energy of the CeO_2 nanoparticles intensifies the effective unification

with the MTO particles that causes a uniform microstructure with large grains. Therefore, the addition of CeO_2 nanoparticles assists the densification and uniform grain growth.

3.3 Effect of Porosity on microwave dielectric properties

In order to comprehend the influence of addition of CeO_2 nanoparticles on MTO ceramics microwave dielectric properties were measured at room temperature and were discussed in our previous study (Bhuyan *et al*. 2013). In the present study, we have calculated the porosity corrected dielectric constants by using the measured microwave dielectric constants for the MTO + *x* CeO_2 nanoparticles(x = 0.00-1.5 wt%) ceramics by using the following equation:

$$\varepsilon_r = \varepsilon_m\left(1-\frac{3P(\varepsilon_m-1)}{2\varepsilon_m+1}\right) \quad (1)$$

where ε_m is the dielectric constant corrected for porosity, $\varepsilon_r$is the experimental dielectric constant, and P is the fractional porosity (Penn *et al*. 1997). The porosity corrected values were bit higher than the experimental values and is tabulated in Table 2.

3.4 Low temperature microwave dielectric measurements:

The variation in resonant frequency of the pure MTO ceramics and MTO ceramics added with different weight percentages of CeO_2 nanoparticles, measured as a function of temperature, is depicted in Fig. 4(a). It is observed that the pure MTO ceramics and the MTO ceramics added with CeO_2 nanoparticles exhibited different resonant frequencies. The distinction in the resonant frequencies is owed to the differences in the real permittivity of the samples and slight variations in the dimensions of the prepared MTO ceramics, with and without the addition of CeO_2 nanoparticles.

Fig. 4(b) shows the variations in the dielectric constants as a function of temperature of the MTO ceramics with and without the addition of CeO_2 nanoparticles. The variations in the dielectric constants over the measured temperature range is very minimal, for example, MTO ceramics added with 1.5 wt% of CeO_2 nanoparticles exhibited the dielectric constant of 12.7 at 6.5K and 12.95 at 295K and the pure MTO exhibited 11.2 at 6.5K and 11.4 at 295K. It was observed that the MTO ceramics added with CeO_2 nanoparticles exhibited higher dielectric constants compared to the pure MTO ceramics. This is due to the differences in the densities of the samples; doped MTO samples have higher densities than the pure MTO samples. The density and microwave dielectric properties of the samples measured at room temperature is shown in Table 3. It is also found that there is a slight variation in the dielectric constants measured at cryogenic temperatures and measured at ambient temperature, and this may be due to the different experimental setups used to measure the dielectric constants (see Table 3).

Fig. 5a shows the temperature dependent of the unloaded Q_u factor of the pure and CeO_2 doped MTO ceramics at approximately 10.35 GHz. It is found that the unloaded Q_u factor first increases partly up to 150 K, then after that it started decreasing with an increase of temperature. The non-monotonous temperature dependences of unloaded Q_u factor below 150 K are seen in most samples, which are caused obviously by extrinsic loss factor and are discussed in the later part. The MTO ceramics doped with CeO_2 nanoparticles exhibited higher unloaded Q_u factor as

compared to pure MTO ceramics. In addition, the sample doped with 1.5 wt% of CeO_2 showed a higher value of Q_u as compared with 0.5 and 1.0 wt% of CeO_2 and the maximum unloaded quality factor (Q_u) of the sample added with 1.5 wt% CeO_2, are 22,000 at 150 K and minimum is 13260 at 295 K. The minimum in unloaded Q_u (T) factor are due to dielectric relaxations which slow down on cooling. The unloaded Q_u factors of the samples measured at ambient temperatures are lower when compared with the unloaded Q_u factors measured at cryogenic temperatures. The difference between ambient measurement and measurement in the controlled environment of the cryogenic system is attributed to humidity, and hence for further discussion only the data obtained with the cryogenic set up is used.

The product of the quality factor and resonant frequency is considered as a tool for evaluating the quality of the dielectric materials. Fig. 5(b) shows the temperature dependent of $Q \times f_0$ of the pure and CeO_2 added MTO ceramics. In all samples, $Q \times f_0$ was increase slightly up to 150 K, after that it started reducing with the increase of temperature. In comparison with pure MTO, the results substantiate that the dielectric properties are improved as a result of addition of CeO_2 nanoparticles The variation in the loss tangent of the pure and doped MTO ceramics as function of temperature is shown in Fig. 5 (c). It is observed that as the temperature increases from 6. 5K to 295K, the loss tangent of the MTO ceramics increased. The loss tangent values for pure MTO ceramics at 6. 5K is 6.66×10^{-5} and at 295K is 9.43×10^{-5} whereas MTO ceramics with 1.5 wt% of CeO_2 nanoparticles exhibited 5.43×10^{-5} at 6.5 and 7.35×10^{-5} at 295K. The MTO ceramics added with higher concentrations (1.0 & 1.5 wt%) of CeO_2 nanoparticles exhibited lower loss tangent compared to the pure and 0.5 wt% CeO_2 added MTO ceramics. This demonstrates that the higher concentration of CeO_2 nanoparticles may be reducing the intrinsic losses, to some extent, extrinsically. The samples with higher concentrations of CeO_2 nanoparticles exhibited higher relative densities and larger grain sizes. So the obtained low loss tangent is attributed to the reduction in both the extrinsic and intrinsic loss mechanisms. The higher loss tangent in the pure and 0.5 wt% CeO_2 added ceramics can be attributed to the lower relative densities and smaller average grain sizes. The dielectric loss arises due to the intrinsic and extrinsic factors. Extrinsic loss occurs due to the secondary phases, chemical in homogeneity, porosity, abnormal grain growth and oxygen deficiency. The extrinsic loss mechanisms are governed by the dipole relaxation of the defect oriented polarization segregated at the grain boundaries. Conversely intrinsic loss mechanism is influenced by the anharmonic forces which facilitates/mediates the interaction between crystal lattice modes and electromagnetic field leading to the damping on optical phonon modes and lattice imperfections, increasing the damping factor (Jacob *et al*. 2007). Further, at low temperatures, the damping of the optical phonon modes or the unharmonocity minimizes The dependence of the loss tangent is expressed as

$$\tan\delta = \frac{\omega\gamma}{\omega^2_T} \tag{2}$$

where γ the damping constant and ω_T isis the resonant frequency of the transverse optical mode which tells that the intrinsic loss is heavily influenced by the temperature because γ is proportional to the temperature (Wakino *et al*. 1986). However, in this study, it is clear that the MTO ceramics with 1.5wt% exhibited low loss tangent compared to the pure MTO which shows that the addition of CeO_2 reduced both extrinsic and intrinsic loss mechanisms. The $Q \times f_o$ values for the 1.5wt% CeO_2 added MTO ceramics measured at microwave frequencies and measured at room temperature also exhibited higher values compared to the other samples (see Table 3). At 1.5 wt%

concentration, the relative density and the average grain sizes are higher compared to the other additive concentrations. Higher the density lowers the porosity and higher average grain size reduces the grain boundary area, and hence the single crystal exhibits the highest Q value (low loss tangent). The microstructures of the MTO ceramics added with 1.0 and 1.5 wt% of CeO_2 nanoparticles reveal the uniform microstructure with larger average grain sizes and higher relative densities governing the microwave dielectric properties of the MTO ceramics especially the loss tangent values.

The temperature coefficient of resonant frequency of the ceramics is estimated using the expression:

$$\tau_f = \frac{f_0 - f_{0T}}{f_0}\frac{10^6}{\Delta T} \tag{3}$$

where f_0 and f_{0T} are the resonant frequencies measured at room temperature and at temperature T, respectively. The temperature coefficient of resonant frequency of the ceramics is known to be influenced by the chemical composition, and the secondary phases present within the material. The variation in the temperature coefficient of frequency of the pure and doped MTO ceramics measured at cryogenic temperatures is shown in Fig. 6a. It is observed that there is not much variation in the temperature coefficient of frequency of the MTO ceramics up to 150K but slight deviation is observed beyond 150 K. Further MTO ceramics added with higher concentrations of CeO_2 nanoparticles exhibited lower values when compared with pure and 0.5 wt% CeO_2 added MTO ceramics. From this study, it is clear that the addition of CeO_2 nanoparticles did not cause any changes on the temperature stability which complements the XRD patterns that there are no secondary phases present in the MTO ceramics up to 1.5 wt% of CeO_2 nanoparticles. The temperature coefficient of permittivity can be calculated using the equation:

$$\tau_\varepsilon = \frac{\varepsilon_0 - \varepsilon_{0T}}{\varepsilon_0}\frac{10^6}{\Delta T} \tag{4}$$

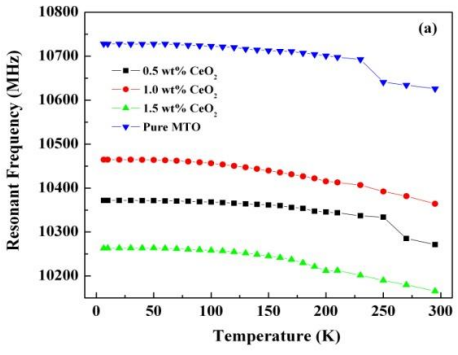

Fig. 4(a) Variation in resonant frequency as a function temperature of the pure MTO and MTO+ *x* CeO_2 (*x = 0.5-1.5* wt.%) ceramics measured

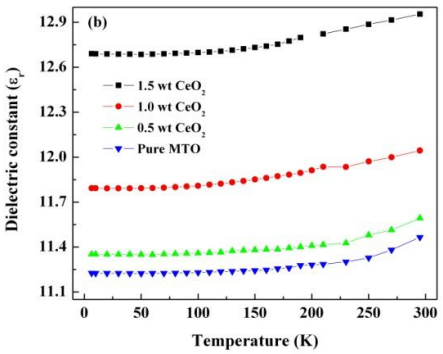

Fig.4(b) Variations in the dielectric constants as a function of temperature of the pure MTO and MTO+ *x* CeO_2 (*x = 0.5-1.5* wt.%) ceramics

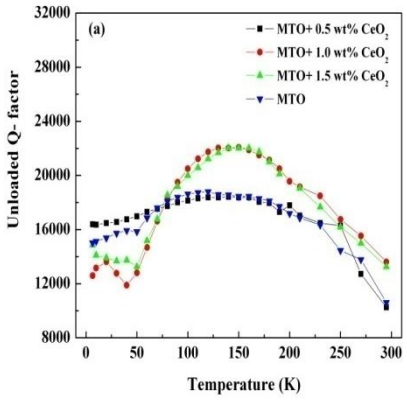

Fig. 5 (a) The unloaded Q factor of the MTO ceramics measured as a function of temperature

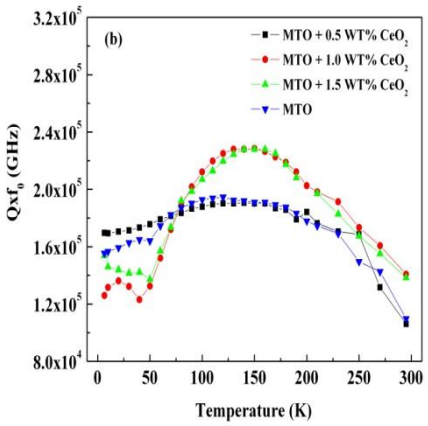

Fig. 5(b) The variation in $Q\times f_0$ of the MTO ceramics as a function of temperature

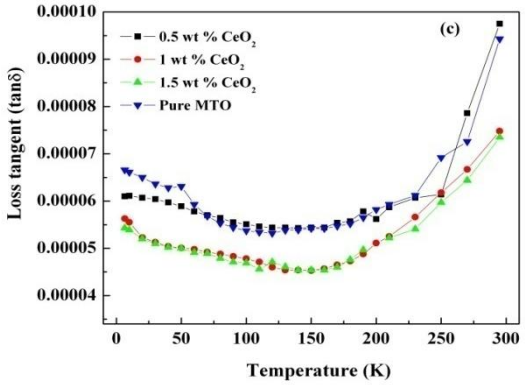

Fig. 5(c) The variation in loss tangent of the MTO ceramics as function of temperature

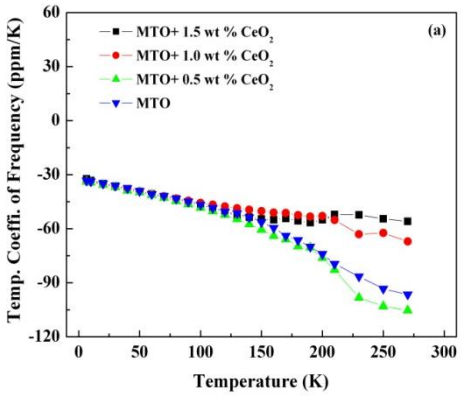

Fig. 6(a). Variation in the temperature coefficient of frequency of the MTO ceramics added with and without CeO_2 nanoparticles

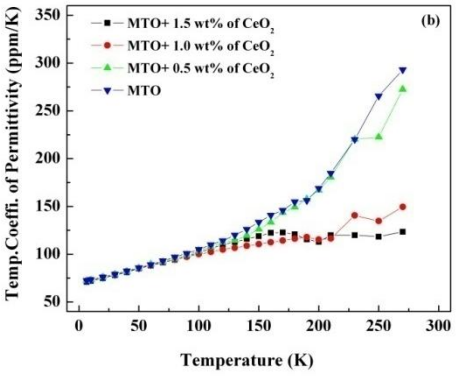

Fig. 6 (b)Variation in the temperature coefficient of frequency of the MTO ceramics added with and without CeO_2 nanoparticles

Table 2Relative density, measured microwave dielectric constant (ε_r) and dielectric constant corrected for porosity (ε_m) values of pure and MTO ceramics added with CeO_2 nanoparticles

Samples name	Sintering temperature	Percentage of density	(ε_r) (measured)	(ε_m) (corrected)
Mg_2TiO_4	1400°C	88.54	11.20	13.22
	1350°C	85.22	10.82	13.95
	1300°C	78.75	10.60	14.88
	1250°C	72.53	10.42	16.71
Mg_2TiO_4+ 0.5 wt% CeO_2 nanoparticles	1400°C	90.32	13.40	15.43
	1350°C	94.12	13.52	14.69
	1300°C	97.13	13.70	14.25
	1250°C	94.50	12.82	13.84
Mg_2TiO_4+ 1.0 wt% CeO_2 nanoparticles	1400°C	91.20	13.72	15.58
	1350°C	95.22	13.85	14.79
	1300°C	97.80	14.26	14.69
	1250°C	95.81	13.00	13.77
Mg_2TiO_4+ 1.5 wt% CeO_2 nanoparticles	1400°C	93.12	13.98	15.40
	1350°C	95.90	14.33	15.17
	1300°C	98.73	14.60	14.85
	1250°C	96.90	13.24	13.81

Table 3Processing condition, relative density, average grain size and the microwave dielectric properties of the MTO ceramics measured at room temperature

Wt% of CeO_2 nanoparticles	Sintering temp. (°C)	Relative Density (%)	Average grain size (μm)	(ε_r) measured at room temp.	$Q \times f_0$(GHz) measured at room temp.
Pure MTO	1400	90.7	3.9	12.8	105500
MTO+0.5 wt% CeO_2 nanoparticles	1300	96.4	7.8	13.7	148000
MTO+1.0 wt% CeO_2 nanoparticles	1300	97.8	10.6	14.2	155500
MTO+1.5 wt% CeO_2 nanoparticles	1300	98.7	11.8	14.6	167000

5. Conclusions

The effect of CeO_2 nanoparticles on the densification, microstructure and microwave dielectric properties were studied systematically. The microwave dielectric properties were measured at cryogenic temperatures. The addition of CeO_2 nanoparticles tailored the microwave dielectric properties of MTO ceramics with improved microstructure and relative density at lower sintering temperatures. The obtained low loss tangent at cryogenic temperatures is held mainly responsible for the reduction in intrinsic losses. The moderation in the loss and temperature dependence of the loss factors with CeO_2 nanoparticles addition in MTO is also attributed to the CeO_2 nanoparticles influencing the intrinsic loss mechanism of MTO. The difference with variation in CeO_2 nanoparticles doping concentration is attributed to extrinsic factors. The MTO ceramics doped with CeO_2 nanoparticles resulted in low loss tangent and moderate dielectric constant with

reasonably stable performance with temperature, which assurances it as a potential material to be used in the devices for microwave communication.

Acknowledgements

The author RKB acknowledges the assistance from DRDO as JRF. The financial support from DRDO [ERIP/ER/0900371/M/01/1264], DAE-BRNS [2010/20/37P/14BRNS], BRFST (NFP-RF-A12-01) and DST [SR/FTP/PS-109/2009] India is greatly acknowledged. The authors acknowledge infrastructure facility (XRD) by DST, New Delhi, through FIST program [SR/FST/PSII-020/2009] is also acknowledged.

References

Belous, A., Ovchar, O., Durylin, D., Valent, M., Krzmanc, M.M. and Suvorov, D. (2007), "Microwave Composite Dielectrics Based on Magnesium Titanates", *J. Euro. Ceram. Soc.*, **27**(8)**,** 2963-2966.

Bhuyan, R.K., Kumar, T.S., Goswami, D., James, A.R., Perumal A. and Pamu, D. (2013), "Enhanced densification and microwave dielectric properties of Mg_2TiO_4 ceramics added with CeO_2 nanoparticles", *Mater. Sci. Eng. B.*, **178**(7), 471-476.

Chen, Y.B. (2012), "Dielectric properties and crystal structure of Mg_2TiO_4 ceramics substituting Mg^{2+} with Zn^{2+} and Co^{2+}", *J. Alloys Compd.*, **513**(5),481-486.

Ferreira, V.M., Baptista, J.L., Kamba, S. and Petzelt, J. (1993), "Dielectric spectroscopy of $MgTiO_3$-based ceramics in the 10^9–10^{14} Hz region", *J. Mater. Sci.*, **28(**21**),** 5894-5900.

Freer, R. and Azough, F. (2008), "Microstructural engineering of microwave dielectric ceramics", *J. Euro. Ceram. Soc.*, **28**(7), 1433-1441.

Ginzton, E.L. (1995), "Microwave Measurements", *McGraw-Hill Book Co*, New York.

Huang, C.L., Chen, J.Y. and Li, B.J. (2010), "A new dielectric material system using (1-x) $(Mg_{0.95}Co_{0.05})_2TiO_4$-$x$ $Ca_{0.8}Sm_{0.4/3}TiO_3$ at microwave frequencies", *Mater. Chem. Phys.*, **120**(1), 217-220.

Jacob, M.V. (2005), "Low temperature microwave characteristics of lithium fluoride at different frequencies," *Sci. Technol. Adv. Mater.*, **6**(8), 944-949.

Jacob, M.V., Mazierskaa, J., Ledenyova, D. and Krupka, J. (2003), " Microwave characterisation of CaF2 at cryogenic temperatures using a dielectric resonator technique", *J. Euro. Ceram. Soc.*, **23(**14**),** 2617-2622.

Jacob, M.V., Hartnett, J.G., Mazierska, J., Krupka, J. and Tobar, M.E. (2006), "Dielectric characterisation of barium fluoride at cryogenic temperatures using TE011 and quasi TE0mn mode dielectric resonators", *Cryogenics*, **46(**10), 730-735.

Jacob, M.V., Mazierska, J., Leong, K. and Krupka, J. (2001), "Simplified method for measurements and calculations of coupling coefficients and Q_0 factor of high temperature super conducting dielectric resonators", *IEEE Trans. Micro. Theory Tech.*., **49**(12), 2401-2407.

Jacob, M.V., Pamu, D. and James Raju, K.C. (2007), "Cryogenic microwave dielectric properties of sintered $(Zr_{0.8}Sn_{0.2})TiO_4$ doped with CuO and ZnO", *J. Am. Ceram. Soc*., **90**(5), 1511-1514.

Kuang, X., Jing, X. and Tang, Z. (2006), "Dielectric loss spectrum of $MgTiO_3$ investigated by AC impedance and microwave resonator measurements", *J. Am. Ceram. Soc*., **89(**1), 241-246.

Pamu, D., Narayana Rao, G.L., Raju James, K.C. and Jacob, M.V. (2007), "Effect of CuO on the sintering and cryogenic microwave characteristics of $(Zr_{0.8}Sn_{0.2})TiO_4$ ceramics", *Sci. Technol. Adv. Mater.*, **8**(6), 469-476.

Penn, S.J., Alford, N.M., Templeton, A., Wang, X., Xu, M., Reece, M. and Schrapel, K. (1997), "Effect of porosity and grain size on the microwave dielectric properties of sintered alumina", *J. Am. Ceram. Soc.*, **80**(7), 1885-1888.

Reaney, I.M. and Iddles, D. (2006), "Microwave dielectric ceramics for resonators and filters in mobile phone networks", *J. Am. Ceram. Soc*., **89(**7), 2063-2072.

Subodh, G., Ratheesh, R., Jacob, M.V. and Sebastian, M.T. (2008), "Microwave dielectric properties and vibrational spectroscopic analysis of $MgTe_2O_5$ ceramics", *J. Mater. Res*., **23**(6), 1551-1556.

Wakino, K., Murata, M. and Tamura, H. (1986), "Far infrared reflection spectra of Ba (Zn,Ta) O_3-$BaZrO_3$ dielectric resonator material," *J. Am. Ceram. Soc*., **69**(1), 34-37.